During muscle atrophy, thick, but not thin, filament components are degraded by MuRF1-dependent ubiquitylation

Shenhav Cohen,[1] Jeffrey J. Brault,[1] Steven P. Gygi,[1] David J. Glass,[3] David M. Valenzuela,[2] Carlos Gartner,[1] Esther Latres,[2] and Alfred L. Goldberg[1]

[1]Department of Cell Biology, Harvard Medical School, Boston, MA 02115
[2]Regeneron Pharmaceuticals, Tarrytown, NY 10591
[3]Novartis Institutes for Biomedical Research, Cambridge, MA 02139

Loss of myofibrillar proteins is a hallmark of atrophying muscle. Expression of muscle RING-finger 1 (MuRF1), a ubiquitin ligase, is markedly induced during atrophy, and MuRF1 deletion attenuates muscle wasting. We generated mice expressing a Ring-deletion mutant MuRF1, which binds but cannot ubiquitylate substrates. Mass spectrometry of the bound proteins in denervated muscle identified many myofibrillar components. Upon denervation or fasting, atrophying muscles show a loss of myosin-binding protein C (MyBP-C) and myosin light chains 1 and 2 (MyLC1 and MyLC2) from the myofibril, before any measurable decrease in myosin heavy chain (MyHC). Their selective loss requires MuRF1. MyHC is protected from ubiquitylation in myofibrils by associated proteins, but eventually undergoes MuRF1-dependent degradation. In contrast, MuRF1 ubiquitylates MyBP-C, MyLC1, and MyLC2, even in myofibrils. Because these proteins stabilize the thick filament, their selective ubiquitylation may facilitate thick filament disassembly. However, the thin filament components decreased by a mechanism not requiring MuRF1.

Introduction

Atrophy of skeletal muscle occurs upon disuse or denervation and systemically in fasting and many disease states, including cancer cachexia, sepsis, renal failure, and cardiac failure (Lecker et al., 1999, 2006; Jackman and Kandarian, 2004). This rapid loss of muscle mass is largely due to accelerated protein degradation, although in systemic catabolic states protein synthesis also decreases (Jackman and Kandarian, 2004; Lecker et al., 2006; Sacheck et al., 2007). Normally, the proteins comprising the myofibril are among the most stable in the body. During atrophy, however, the myofibrillar apparatus, which comprises at least 60% of muscle proteins, decreases in mass to a greater extent than the soluble components (Munoz et al., 1993) and results in decreased strength. The present studies were undertaken to gain insight into the mechanisms responsible for this accelerated degradation of myofibrillar proteins.

Recent findings indicate that these different types of atrophy activate a common series of biochemical and transcriptional adaptations (Sacheck et al., 2007) leading to enhanced protein degradation by both proteasomal and lysosomal systems (Mammucari et al., 2007; Zhao et al., 2007). The degradation of myofibrillar components during atrophy is mediated by the ubiquitin–proteasome pathway (Solomon and Goldberg, 1996). Despite this rapid degradation of diverse muscle proteins during atrophy, two muscle-specific ubiquitin ligases (E3s), muscle RING-finger 1 (MuRF1) and atrogin-1/MAFbx, are markedly induced; and in knockout mice lacking either enzyme, the rapid loss of muscle mass upon denervation is significantly reduced (Bodine et al., 2001; Gomes et al., 2001). To date, it is unclear whether these E3s ubiquitylate many muscle components or only key regulatory ones, whose destruction promotes the breakdown of other proteins. MuRF1 is a monomeric E3 belonging to the tripartite motif family of ligases which contain a tripartite RING:B-box:coiled-coil domain that is essential for ubiquitin conjugation. Two close homologues of MuRF1 (MuRF2 and

Correspondence to Alfred L. Goldberg: alfred_goldberg@hms.harvard.edu

Abbreviations used in this paper: MyBP-C, myosin-binding protein C; MyHC, myosin heavy chain; MyLC, myosin light chain; MuRF, muscle RING-finger; WT, wild type.

The Rockefeller University Press $30.00
J. Cell Biol. Vol. 185 No. 6 1083–1095
www.jcb.org/cgi/doi/10.1083/jcb.200901052

MuRF3) are present in normal muscle and appear to be important for maintenance of normal contractile function (Fielitz et al., 2007; Witt et al., 2008). MuRF1, on the other hand, is required for rapid atrophy but not for normal muscle growth.

In the present studies, we have used mice that lack MuRF1's RING domain to clarify the role of its ligase activity in denervation atrophy. Although two substrates have been reported for MuRF1, cardiac Troponin-I (Kedar et al., 2004) and myosin heavy chain (MyHC) (Clarke et al., 2007), the role of MuRF1 in degrading specific myofibrillar or soluble proteins in skeletal muscle is unknown. Specifically, it is unclear whether MuRF1 or any E3 can act on the proteins within the myofibril, which is a highly organized rigid structure, or whether mechanisms exist to release proteins from the sarcomeres before ubiquitin-dependent degradation. Model studies in muscle extracts have demonstrated rapid hydrolysis of purified actin and myosin by the ubiquitin–proteasome pathway (Solomon and Goldberg, 1996). However, these proteins were much more stable when associated with each other in the actomyosin complex or intact myofibrils. These findings raised the possibility that the ubiquitin–proteasome system may not by itself be able to degrade components of intact myofibrils, and constituent proteins have to be released by some mechanism to be substrates for degradation (Solomon and Goldberg, 1996). Consequently, several groups have presented evidence that a calpain (Tidball and Spencer, 2002) or caspase (Du et al., 2004) may initially cleave the myofibrillar components, thereby accelerating disassembly and degradation by the ubiquitin–proteasome system. However, direct proof of these models functioning in atrophying muscles is lacking. Alternatively, an E3 may act directly on specific components of the myofibril to promote its disassembly and degradation during atrophy. Here, we present evidence for such a role for MuRF1.

Myofibrils are composed of precisely aligned filament systems arranged in repeating units of sarcomeres (Clark et al., 2002), whose primary constituents are myosin in the thick filament and actin in the thin filament. The myosin molecule comprises 50% of myofibrillar mass and contains two heavy chains, two regulatory light chains (MyLC2), and two essential light chains (MyLC1). These light chains bind to the globular heads of myosin, which comprise the cross-bridges that extend from the thick filaments to interact with actin and generate force through ATP hydrolysis. Several observations in vivo and with isolated myofibrils indicate that MyLC1 and MyLC2 are required for thick-filament stabilization and normal contractility. Loss of MyLC1 or MyLC2 in humans (Rottbauer et al., 2006) or their homologues in zebrafish (Chen et al., 2008) results in a perturbation of contractility and a striking disorganization of the thick filaments.

In addition, the sarcomere contains many structural and regulatory proteins that contribute to myofibril integrity and stability. For example, myosin-binding protein C (MyBP-C) is a component of the thick filament and is distributed every 43 nm within the C-zone of the sarcomere, where the cross-bridges are found (Offer et al., 1972). Transgenic mice expressing truncated MyBP-C that lacks the myosin-binding site in cardiac muscle exhibit significant sarcomere disorganization (Yang et al., 1998). Because MyBP-C, MyLC1, and MyLC2 are required for sarcomere stability, their selective loss and rapid ubiquitylation, which we demonstrate here, are likely to be a mechanism promoting myofibrillar disassembly during atrophy.

In these studies, we used biochemical and genetic approaches to clarify in vivo the contribution of MuRF1's ligase activity to the atrophic process and to clarify MuRF1's role in disassembly of the myofibrillar apparatus in adult mice. Specifically, we investigated (1) whether any myofibrillar protein may be lost selectively during denervation atrophy, (2) whether ubiquitylation by MuRF1 is important for the degradation of the various myofibrillar proteins lost during atrophy, (3) whether MuRF1 can ubiquitylate regulatory proteins, whose loss may promote the breakdown of other myofibrillar components, and (4) whether myofibrillar proteins that are degraded in a MuRF1-dependent mechanism can be ubiquitylated within the myofibril, in the extracted actomyosin complex, or only when isolated and purified. These studies surprisingly demonstrate that distinct mechanisms exist for degrading components of the thick and thin filaments, and that certain thick filament–associated proteins are lost differentially during atrophy and are selectively ubiquitylated within the intact myofibril. Their differential loss may represent a critical step that promotes further ubiquitylation and degradation of other myofibrillar components.

Results

MuRF1 binds a specific subset of muscle proteins

To understand the role of MuRF1 in muscle atrophy, we sought to identify its substrates. Soluble extracts of gastrocnemius muscles from normal mice (the 3,000 *g* supernatant) were incubated with immobilized GST-MuRF1 to isolate those muscle proteins having high affinity for MuRF1. The resulting precipitates were washed extensively with buffer containing 500 mM NaCl to remove nonspecific or weakly associated proteins. The proteins on the pellets were analyzed by SDS-PAGE (Fig. S1) and mass spectrometry. Many myofibrillar components, especially components of the thick filaments and M-line region, were identified (Table I), including myosin-binding protein C (MyBP-C, also called C-protein), myosin essential light chain (MyLC1) and regulatory light chain (MyLC2), myosin heavy chain (MyHC) type II isoform, myomesin 1, and filamin C (also called filamin 2, γ-filamin, or ABP-L), a component localized to the Z-disk. This binding of MyLC2 is consistent with the results of screening a muscle cDNA library for MuRF1-binding proteins by a yeast two-hybrid assay (Witt et al., 2005). Furthermore, MyHC (Clarke et al., 2007) has been shown to be ubiquitylated by purified MuRF1. We could not precipitate Troponin-I from skeletal muscle extracts with MuRF1, although cardiac Troponin-I is reported to be a substrate of MuRF1 in vivo (Kedar et al., 2004), and is readily ubiquitylated by purified MuRF1 (Kim et al., 2007).

To confirm that these MuRF1-binding proteins (Table I) are indeed potential substrates, we repeated the isolation of proteins together with purified GST-MuRF1 from normal gastrocnemius muscles and subsequently tested if these bound components could be ubiquitylated after addition of E1, UbcH1,

Table I. **MuRF1 binds a variety of myofibrillar proteins present in muscle homogenate (3,000 *g* supernatant)**

Protein name	Gene	Gene ID (NCBI)	Precipitated from normal muscle with pure MuRF1	Ubiquitylated after addition of E1, E2, and ATP	Immunoprecipitated from denervated muscle with Myc-ΔR-MuRF1
MyBP-C	Mybpc2	233199	+	+	+
Myosin regulatory light chain (MyLC2)	Mylpf	17907	+	+	+
Myosin essential light chain (MyLC1)	Myl1	17901	+	+	+
Myosin heavy chain 1	Myh1	17879	+	+	+
Myosin heavy chain 4	Myh4	17884	+		+
Myosin heavy chain 8	Myh8	17885	+		+
Myomesin 1	Myom1	17929	+		+
Actin, alpha skeletal muscle	Acta1	11459	+	+	+
Filamin C, gamma isoform 1	Flnc	68794	+		+

MuRF1-bound proteins were immunoprecipitated together with MuRF1 from gastrocnemius muscles and identified by mass spectrometry. When a subsequent in vitro ubiquitylation was applied, mass spectrometry analysis identified MyBP-C, MyLC 1 and 2, MyHC, actin, and myomesin as ubiquitylated species.

and His-ubiquitin. The His-tagged polyubiquitylated proteins were purified with a nickel column, and mass spectrometry analysis identified all of these myofibrillar proteins as species ubiquitylated by MuRF1 (Table I).

Generation of MuRF1 knock-in mice expressing MuRF1 or a MuRF1-RING deletion mutant

To confirm that these proteins are MuRF1's substrates during atrophy in vivo, we generated two lines of knock-in mice expressing Myc epitope-tagged MuRF1, one expressing the full-length MuRF1 (Myc-MuRF1) and a second line that expressed MuRF1 lacking its Ring-finger domain (Myc-ΔR-MuRF1). Because the Ring-finger domain is required to catalyze ubiquitylation (Hatakeyama and Nakayama, 2003), but not for interaction with substrates, in the Myc-ΔR-MuRF1 strain, the proteins ubiquitylated by MuRF1 upon denervation should escape rapid degradation but still can bind to Myc-ΔR-MuRF1, which should greatly facilitate their identification by mass spectrometry. Similar approaches have been successfully used in vitro to identify the substrates of other RING-finger E3s (Qiu and Goldberg, 2002; Jang, 2004). To generate MuRF1$^{myc/myc}$ and ΔR-MuRF1$^{myc/myc}$ mice, we engineered two targeting vectors: one that would result in the addition of a Myc epitope sequence at the N terminus of MuRF1, and one that additionally would remove the Ring-finger domain (Fig. 1). Targeting vectors were inserted into the mouse genome via targeted replacement by homologous recombination. The heterozygous MuRF1$^{+/myc}$ and ΔR-MuRF1$^{+/myc}$ mice were identified by real-time PCR-based loss of native allele (LONA) assay and were then used to generate the homozygous mice used in our experiments (Fig. S2). The homozygous MuRF1$^{myc/myc}$ and ΔR-MuRF1$^{myc/myc}$ mice showed no gross abnormalities and did not appear in any way different from either the wild-type (WT) or MuRF1$^{-/-}$ mice.

Effects of Myc-ΔR-MuRF1 on muscle atrophy

To analyze the regulation of Myc-MuRF1 and Myc-ΔR-MuRF1 expression during atrophy, we sectioned unilaterally the sciatic nerve in the two groups of mice. 10 d later the animals were killed, and extracts of the gastrocnemius muscles were prepared. Marked induction of Myc-MuRF1 protein in these lysates was observed by Western blot and resembled the induction of MuRF1 in WT mice (Fig. 1 B). Interestingly, the content of Myc-ΔR-MuRF1 in the denervated muscles was higher than the content of MuRF1 in WT mice (Fig. 1 D), probably because like many E3s, MuRF1 autoubiquitylates, and in the absence of the Ring-finger domain, the protein is inactive and consequently much more stable (Qiu and Goldberg, 2002). Even though it lacks the RING domain (55 amino acids), the expressed Myc-ΔR-MuRF1 protein was very similar in size to the endogenous MuRF1 because it contains a Myc tag (36 amino acids). As expected, the size of the Myc-MuRF1 protein was greater than that of the Myc-ΔR-MuRF1 because of the presence of the RING domain.

To determine if MuRF1's ubiquitin ligase activity was essential for atrophy and degradation of specific myofibrillar proteins, we analyzed the rate of denervation atrophy to learn if deletion of MuRF1's Ring-finger reduced atrophy in a similar fashion as a complete MuRF1 deletion (Bodine et al., 2001). Unilateral atrophy of the hindlimb muscles was induced by cutting the right sciatic nerve in the MuRF1$^{-/-}$, MuRF1$^{myc/myc}$, and ΔR-MuRF1$^{myc/myc}$ in three separate experiments with WT littermates from each cohort as controls (n = 5–8). The gastrocnemius muscles of both limbs were dissected and weighed 14 d later. As reported previously (Bodine et al., 2001), these muscles in the WT lost ∼35% of their mass, but only 20% in the MuRF1$^{-/-}$ ($P < 0.001$; unpublished data). The gastrocnemius muscles of mice expressing full-length Myc-MuRF1 decreased in weight to a similar extent as in WT (36% vs. 41%, respectively; Fig. 1 E). In contrast, the muscles expressing the nonfunctional Myc-ΔR-MuRF1 decreased in weight by only 22% (which resembled the 20% decrease in the MuRF1$^{-/-}$) compared with the 38% decrease in WT littermates ($P < 0.01$; Fig. 1 E). Thus, MuRF1's Ring-finger domain (i.e., its function as a ubiquitin ligase) is essential for rapid atrophy after denervation, and loss of this domain is equivalent to the loss of the entire protein.

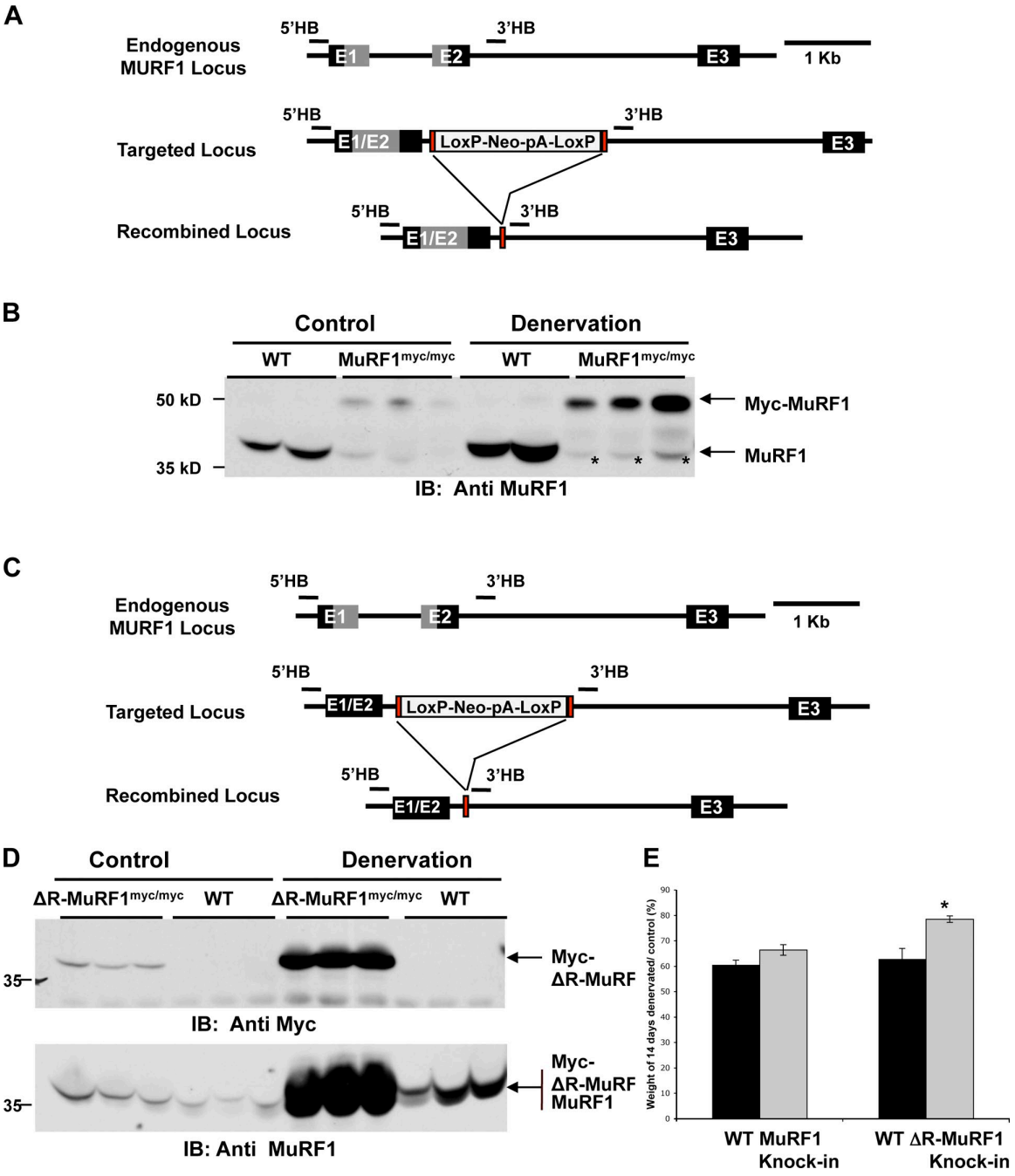

Figure 1. **Targeted replacement of MuRF1 with Myc-MuRF1 or Myc-ΔR-MuRF1 and their expression in skeletal muscle after denervation.** (A) Strategy for the generation of MuRF1$^{myc/myc}$ mice showing the Ring-finger domain (gray box) spanning the first two exons of *MuRF1* (endogenous locus). The targeting cassette was generated by replacing the firsts two exons (E1 and E2) of *MuRF1* with a Myc-encoding sequence fused in-frame with the region of *MuRF1* encoding D2-S110, followed by a short intron sequence, and a selectable marker (NEO, neomycin resistance gene) (targeted locus). Upon homologous recombination, the floxed NEO cassette was removed with a Cre expression vector (recombined locus). (B) Immunoblot analysis of MuRF1 in gastrocnemius muscle from adult wild-type mice (WT) and Myc-MuRF1 from MuRF1$^{myc/myc}$ littermates after 10 d of denervation. The muscles on the right hindlimb were denervated by cutting the sciatic nerve, and the left hindlimb muscles of each animal served as the control. A MuRF1 antibody was used for Western blot. Asterisks indicate nonspecific bands. (C) Strategy for the generation of ΔR-MuRF1$^{myc/myc}$ mice showing the Ring-finger domain (gray box) spanning the first two exons of MuRF1 (endogenous locus). The targeting cassette was generated by replacing the first two exons (E1 and E2) of *MuRF1* with a Myc-encoding sequence fused in-frame with the region of *MuRF1* encoding D2-S110 without the sequence corresponding to the Ring-finger domain C23-C78, followed by a short intron sequence, and a selectable marker (NEO, neomycin resistance gene) (targeted locus). Upon homologous recombination, the floxed NEO gene was removed using a Cre expression vector (recombined locus). (D) Immunoblot analysis of MuRF1 in gastrocnemius muscle from WT mice and of ΔR-Myc-MuRF1 in muscles from ΔR-MuRF1$^{myc/myc}$ littermates 10 d after denervation. Antibodies used for Western blot are indicated. (E) Denervation atrophy of gastrocnemius in WT and MuRF1$^{myc/myc}$ or ΔR-MuRF1$^{myc/myc}$ mice. Weight of gastrocnemius in MuRF1$^{myc/myc}$ animals decreased 14 d after denervation to a similar extent as in WT littermates. By contrast, muscle weight from ΔR-MuRF1$^{myc/myc}$ animals decreased to a lesser extent than in WT littermates (*, $P < 0.01$). Weights of denervated muscles are expressed as percentage of the contralateral control. Error bars represent SEM ($n = 7$) versus innervated muscles from WT.

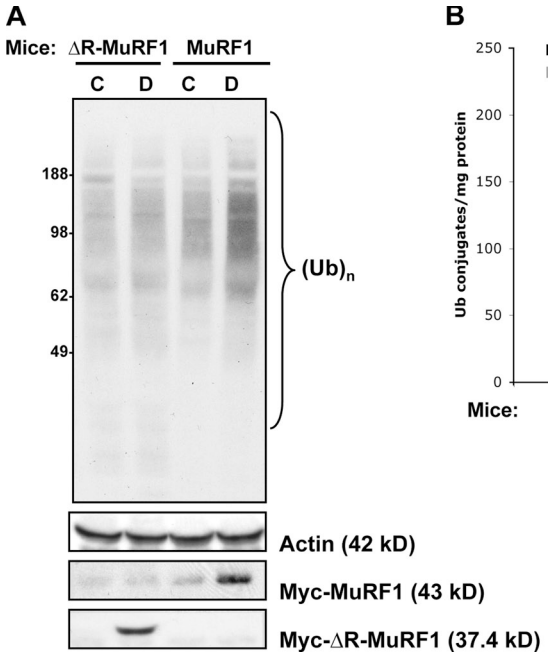

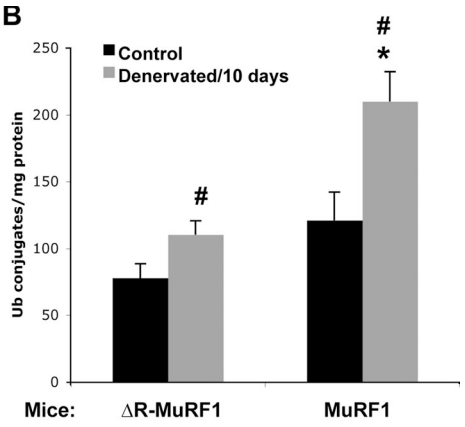

Figure 2. **MuRF1 is responsible for most of the increase in total ubiquitin conjugates during denervation atrophy.** (A) The cytosolic fractions (20 µg) of 10-d denervated or control gastrocnemius muscles from MuRF1$^{myc/myc}$ and ΔR-MuRF1$^{myc/myc}$ mice were subjected to immunoblotting with an antibody against polyubiquitin conjugates. The membrane was re-probed with anti-actin to ensure equal protein loading. C, control; D, denervation for 10 d. (B) Densitometric analysis of Western blot presented in A, with mean given as arbitrary units. Error bars represent SEM, $n = 4$. #, $P < 0.001$ versus innervated muscles; *, $P < 0.05$ versus denervated muscles from ΔR-MuRF1$^{myc/myc}$ mice.

MuRF1 has been reported to be associated with myofibrils (Centner et al., 2001), although an immunofluorescence study on cardiac myocytes detected MuRF1 also in the cytoplasm (McElhinny et al., 2002). After isolation of myofibrils from gastrocnemius muscles of the MuRF1$^{myc/myc}$, ΔR-MuRF1$^{myc/myc}$, and WT mice, we found to our surprise that the great majority of Myc-MuRF1 and Myc-ΔR-MuRF1 and endogenous MuRF1 in WT mice were in the cytosolic fraction (3,000 *g* supernatant) (Fig. S3). Therefore, if MuRF1 is in fact associated with the myofibrils, it is a weak, easily disrupted interaction.

To identify the MuRF1 substrates lost upon denervation in vivo, we immunoprecipitated Myc-ΔR-MuRF1 from gastrocnemius muscles (3,000 *g* supernatant) from homozygous ΔR-MuRF1$^{myc/myc}$ mice using antibodies against its Myc tag, and washed the resulting immunoprecipitates as described above. Analysis of MuRF1-bound proteins by mass spectrometry identified the same set of myofibrillar proteins that were precipitated using immobilized GST-MuRF1 (Table I).

MuRF1 is responsible for most of the increase in ubiquitin conjugates after denervation

Wing et al. (1995) previously demonstrated that the muscle's content of ubiquitin conjugates is significantly increased during denervation atrophy. We therefore examined whether this accumulation of ubiquitylated proteins depends on MuRF1 function. In accord with prior findings on rat muscles, in mouse muscles expressing Myc-MuRF1 10 d after denervation, the gastrocnemius's content of ubiquitin conjugates was 73% higher ($P < 0.001$) than in control muscles, as shown by immunoblotting of the cytosolic fraction with an antibody against ubiquitin chains (Fig. 2). However, in ΔR-MuRF1$^{myc/myc}$ mice, a much smaller increase (by 42%; $P < 0.05$) in ubiquitin conjugates was observed in denervated muscles than in controls (Fig. 2). Thus, MuRF1's ligase activity appears responsible for most of the increase in total ubiquitin conjugates 10 d after denervation and probably for much of the increased proteolysis. The inability of muscles in the ΔR-MuRF1$^{myc/myc}$ mice to increase ubiquitylation can account for their reduced rate of atrophy.

MyLC1, MyLC2, and MyBP-C are selectively lost during denervation atrophy by a MuRF1-dependent mechanism

To clarify the role of MuRF1 in denervation atrophy and to investigate if any of these sarcomeric proteins are lost differentially during this process, we isolated myofibrils from gastrocnemius muscles, and after SDS-PAGE identified the constituent protein bands by Coomassie blue staining and mass spectrometry (Fig. S4 A). We then analyzed by SDS-PAGE equal amounts of proteins from the myofibrillar fraction of innervated and denervated muscles from the MuRF1$^{myc/myc}$ and ΔR-MuRF1$^{myc/myc}$ mice and measured the intensity of specific bands stained with Coomassie blue by densitometry (Fig. S4 B). Muscle weights in ΔR-MuRF1$^{myc/myc}$ and MuRF1$^{myc/myc}$ animals decreased similarly (14% [$P < 0.05$] vs. 18% [$P < 0.001$], respectively) 10 d after denervation (unpublished data). Despite the loss of proteins, the relative concentrations of the great majority of myofibrillar proteins at 10 d denervation did not differ significantly from those in the innervated muscles (Fig. 3 A).

Surprisingly, in animals expressing Myc-MuRF1, the relative concentrations of myofibrillar MyLC2 and MyBP-C were markedly decreased (by 47% and 28%, respectively; $P < 0.05$) below levels the innervated controls (Fig. 3 A). By contrast, in ΔR-MuRF1$^{myc/myc}$ mice the relative amounts of these regulatory proteins did not change significantly after denervation (Fig. 3 A) (this decrease in the amount of MyBP-C is not due to the slow-to-fast change in fiber type that occurs after denervation [Weydert et al., 1987] because the fast and slow isoforms of MyBP-C have the same molecular mass and appear as one band on Coomassie blue–stained gels). This differential loss of

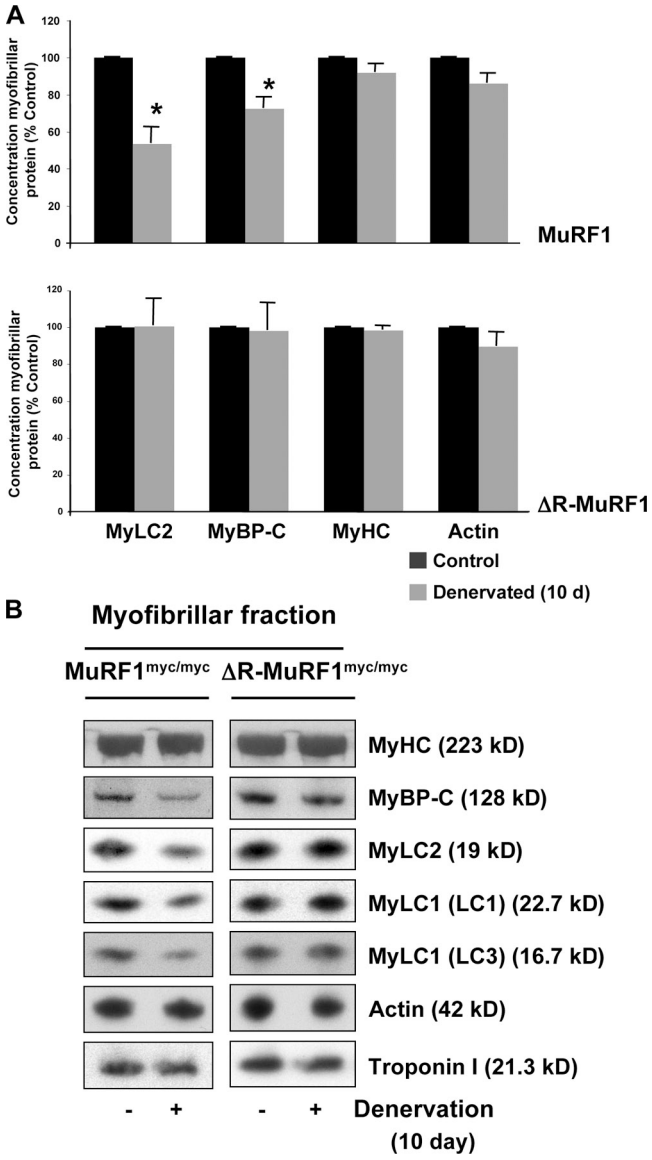

Figure 3. **By 10 d denervation, MyLC1, MyLC2, and MyBP-C are selectively lost by a MuRF1-dependent mechanism.** The myofibrillar fractions from 10-d denervated and control gastrocnemius muscles from both MuRF1$^{myc/myc}$ and ΔR-MuRF1$^{myc/myc}$ mice were analyzed by SDS-PAGE, Coomassie blue staining, and densitometric measurement of the specific bands. (A) The concentration of each protein per mg myofibrillar protein for denervated muscles is expressed as a percentage of the mean intensity in innervated controls. Error bars represent SEM, $n = 3$. *, $P < 0.05$ versus innervated muscles. (B) The myofibrillar fraction (0.5 µg) from denervated and innervated muscles from both types of mice was analyzed by SDS-PAGE and immunoblotted with specific antibodies as indicated.

MyLC2 and MyBP-C is noteworthy because the concentrations of MyHC and actin in the myofibrils were unchanged in denervated muscles from both groups.

Because MyLC1 and Troponin-I migrate similarly on SDS-PAGE, their concentrations could not be measured by this method. Instead, we analyzed their levels by immunoblotting (Fig. 3 B). Like MyLC2 and MyBP-C content, the level of MyLC1 was lower in the myofibrillar fraction of the denervated muscle than the innervated muscle from MuRF1$^{myc/myc}$ mice but did not decrease in ΔR-MuRF1$^{myc/myc}$ animals (Fig. 3 B). We also confirmed by immunoblotting that the relative concentrations of myofibrillar MyHC and actin did not differ in the denervated and innervated muscles at this time (Fig. 3 B). By contrast, the content of Troponin-I, whose cardiac isoform is ubiquitylated by MuRF1 and degraded in cultured cardiomyocytes (Kedar et al., 2004), was unchanged at 10 d denervation. Together, these data indicate that myofibrillar MyLC1, MyLC2, and MyBP-C are preferentially degraded during denervation atrophy in a MuRF1-dependent mechanism, but other potential substrates of MuRF1 (e.g., the thin filament component, Troponin-I) are not.

MyLC1, MyLC2, and MyBP-C are also lost differentially upon fasting

To determine if selective loss of regulatory proteins also occurs during other types of muscle wasting, we tested whether MyLC1, MyLC2, and MyBP-C are also selectively degraded upon food deprivation where there is also rapid atrophy and MuRF1 induction. Mice fasted for 2 d showed a 12% decrease in muscle weight, a similar decrease in MyHC content, and a 24% decrease in actin content ($P < 0.05$) (Fig. S5 A, left). In contrast, MyBP-C and MyLC2 content decreased by almost 40% in these muscles ($P < 0.001$). Immunoblotting for MyLC1 confirmed a similar preferential loss (Fig. S5 A, right). The significant decrease in actin content at the second day of fasting was not apparent at 10 d denervation (Fig. 3 A), and thus may imply for the differences between disuse (e.g., denervation) and systemic catabolic states (e.g., fasting) in rates of muscle atrophy or signaling pathways leading to degradation. In any case, the ratio of MyBP-C and MyLC2 to actin falls in the gastrocnemius by 2 d of food deprivation (Fig. S5 B). Thus, a similar selective loss of MyLC1, MyLC2, and MyBP-C occurs upon food deprivation as during denervation atrophy.

MyLC1, MyLC2, and MyBP-C (unlike MyHC) can be ubiquitylated in the actomyosin complex

To confirm that MyLC1, MyLC2, and MyBP-C are direct substrates for MuRF1, we measured their ubiquitylation by recombinant MuRF1 using different E2s and Western blot analysis (Fig. 4). MuRF1 ubiquitylated pure MyLC1 (Fig. 4 A), MyLC2 (Fig. 4 B), and MyBP-C (Fig. 4 C), as well as MyHC (Fig. 4 D) with the three E2s tested, UbcH1, UbcH5, or UbcH13/Uev1, all of which were previously shown to support ubiquitylation of cardiac Troponin-I by MuRF1 (Kim et al., 2007). Actin is mainly monoubiquitylated by MuRF1 and UbcH5 (Fig. S5 C), although in vivo this chain may be elongated by a different ubiquitin ligase, functioning as an E4 (Koegl et al., 1999) or by MuRF1 with a different E2 (as recently suggested for targets of the anaphase-promoting complex [Rodrigo-Brenni and Morgan, 2007]).

Solomon and Goldberg (1996) had previously shown that when actin and myosin were in the myofibril or even in actomyosin complexes, these proteins were quite resistant to ubiquitin-dependent proteolysis, unlike free actin or myosin (Solomon and Goldberg, 1996). To learn whether MuRF1 can directly ubiquitylate proteins in the myofibril, or whether this structure

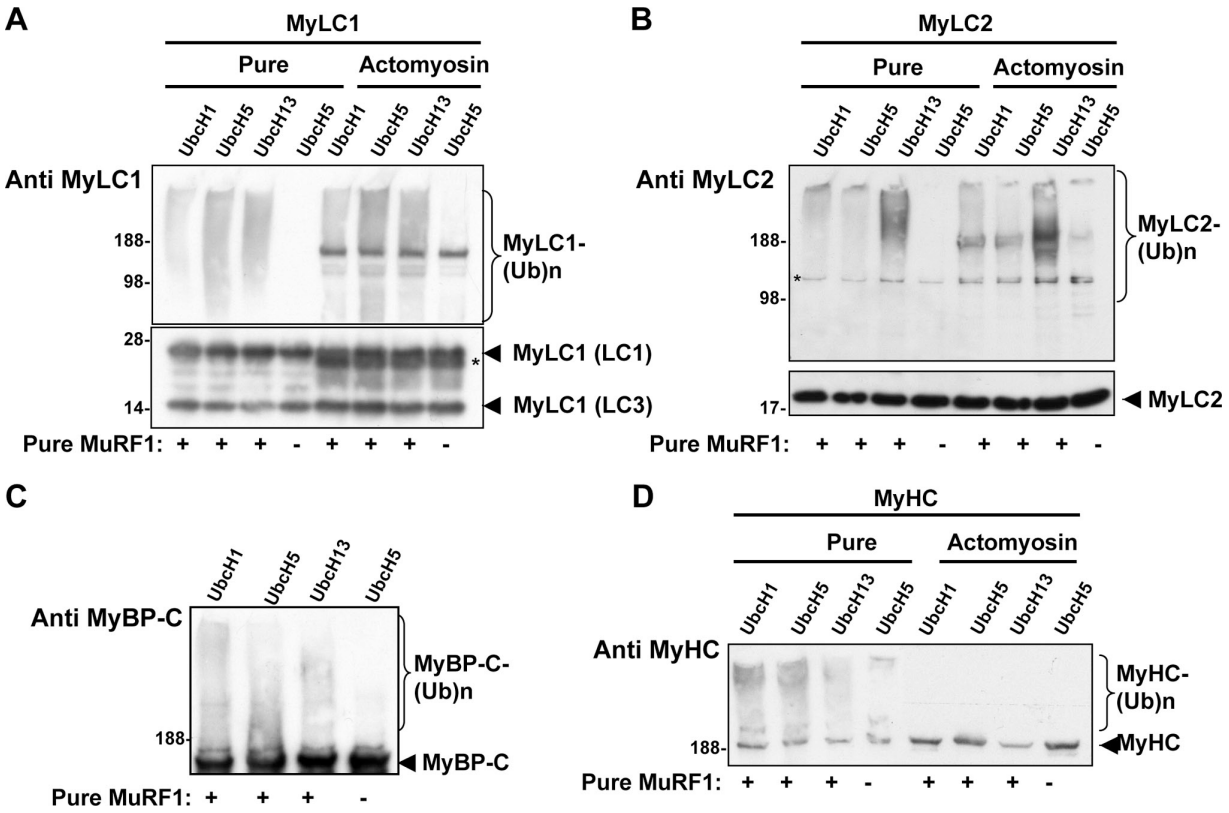

Figure 4. **Pure MyLC1, MyLC2, MyBP-C, and MyHC are substrates of MuRF1, but in the actomyosin complex MyHC is not efficiently ubiquitylated.** In vitro ubiquitylation of actomyosin complex or pure MyLC1 (A), MyLC2 (B), MyBP-C (C), and MyHC (D) by MuRF1 and three different E2s (UbcH13/Uev1). We assayed similar concentrations of pure MyHC and in association within actomyosin (as determined by Coomassie blue–stained gels). Asterisk indicates a nonspecific band. Dividing lines were used to separate top and bottom parts of the gel.

must first be dissociated, we investigated whether MyLC1 and MyLC2 associated in actomyosin complexes are also substrates for ubiquitylation by MuRF1 (we could not measure ubiquitylation of MyBP-C in actomyosin because it is not present in the actomyosin preparation). We compared ubiquitylation of pure proteins and in parallel an actomyosin preparation from rabbit muscle (which in addition to actin, MyHCs, and MyLCs may contain low amounts of associated proteins, e.g., tropomyosin, troponin, α-actinin). Similar amounts of each of the proteins were present in the reactions, either as pure protein or in association with actomyosin (adjusted after we determined the amounts of each protein by Coomassie blue staining of gels). MuRF1 ubiquitylated MyLC1 and MyLC2 in the actomyosin complex at comparable rates as the free proteins with all three E2s tested (Fig. 4, A and B). By contrast, MyHC could be ubiquitylated only as pure protein but not when associated within actomyosin complex (Fig. 4 D).

MyLC1, MyLC2, and MyBP-C can also be ubiquitylated in the myofibril

To test whether MyLC1, MyLC2, and MyBP-C are also efficiently ubiquitylated when associated within the myofibril, we unilaterally denervated gastrocnemius muscles from WT mice for 3 or 10 d, prepared myofibrils from these and the contralateral normal muscles, and compared rates of ubiquitylation of proteins in the myofibrils by pure MuRF1. As observed in the MuRF1$^{myc/myc}$ animals, MyLC2 and MyBP-C were preferentially lost (relative to actin) from the gastrocnemius by 10 d after denervation, whereas the relative concentration of MyHC was unchanged (Fig. 5 A, left). In addition, immunoblotting revealed lower levels of MyLC1 in the myofibril from denervated muscle than in the control (Fig. 5 A, right).

A specific immunoprecipitation assay was established to isolate ubiquitylated proteins and analyze them by immunoblotting. To assay ubiquitylation of proteins in myofibrils from normal or denervated muscles by MuRF1, we used 6-His–tagged ubiquitin, UbcH1, and E1. After incubation at 37°C, 5 M urea was added to disassemble the myofibrils and permit efficient purification of the His-ubiquitylated material with a nickel column. When isolated myofibrils from normal mice were incubated with MuRF1, no significant ubiquitylation of actin or MyHC could be demonstrated by immunoblotting (unpublished data). By contrast, MyLC1, MyLC2, and MyBP-C within the myofibril were efficiently ubiquitylated in both control and denervated muscles (Fig. 5 B). Thus, in the intact myofibril and even in the actomyosin complex, MyHC and actin (unlike MyLC1, MyLC2, and MyBP-C) show only limited susceptibility to ubiquitylation, i.e., much less than purified MyHC and actin. Because MyLC1, MyLC2, and MyBP-C are known to stabilize the thick filaments, their differential ubiquitylation and degradation may facilitate the ubiquitylation, disassembly, and degradation of other sarcomeric components.

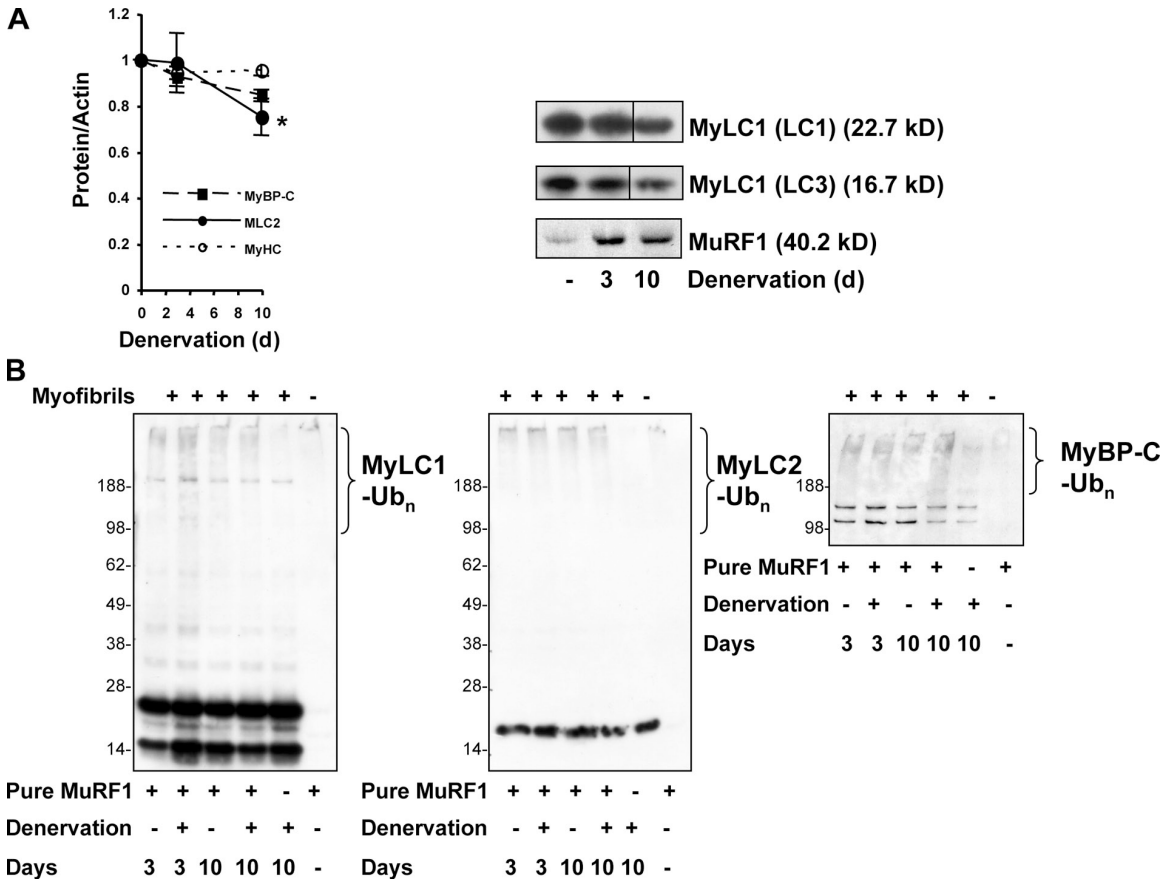

Figure 5. **MyBP-C and MyLCs are lost selectively during atrophy and are efficiently ubiquitylated by MuRF1 in isolated myofibrils.** (A) Equal amounts of the myofibrillar fraction from innervated gastrocnemius muscles and ones denervated for 3 or 10 d from WT mice were analyzed by SDS-PAGE and Coomassie blue staining (left). The intensity of specific Coomassie blue–stained bands was measured, and the ratio to actin was plotted. Error bars represent SEM, $n = 5$. *, $P < 0.05$. Shown on the right is Western blot analysis of myofibrillar fraction (0.5 µg, to detect MyLC1) and cytosolic fractions (20 µg, to detect MuRF1) from innervated and denervated muscles from WT mice. (B) MyBP-C and MyLCs are ubiquitylated by purified MuRF1 in isolated myofibrils from control muscles and ones denervated for 3 or 10 d using UbcH1 and His-tagged ubiquitin. His-Ubiquitylated proteins were purified with a nickel column and detected by immunoblotting with specific antibodies.

Actin and other thin filament components were subsequently lost independently of MuRF1

It has often been proposed that an initial disassembly step, such as a proteolytic cleavage by calpains (Goll et al., 1992) or caspases (Du et al., 2005) may facilitate the overall degradation of the myofibrillar apparatus. However, we showed above that MyLC1, MyLC2, and MyBP-C are preferentially lost during denervation atrophy by a MuRF1-dependent mechanism (Fig. 3) and can be ubiquitylated by MuRF1 when still associated with the myofibril (Fig. 5 B). Furthermore, purified soluble actin and MyHC are ubiquitylated by MuRF1 more efficiently than when these proteins are associated with other components within the myofibril or even in the actomyosin complex (Fig. 4). These findings raise the possibility that the loss of MyLC1, MyLC2, and MyBP-C may enhance the susceptibility of other myofibrillar components to MuRF1-dependent degradation.

To examine this hypothesis, we measured the content of thick and thin filament components 14 d after denervation. Control and denervated muscles from MuRF1$^{myc/myc}$ and ΔR-MuRF1$^{myc/myc}$ mice were homogenized, and isolated myofibrils were analyzed by SDS-PAGE and Coomassie blue staining. Measurement of the intensity of specific bands revealed the differential loss of MyHC from the myofibril at 14 d denervation in MuRF1$^{myc/myc}$ mice (Fig. 6 A), which was not evident 10 d after denervation (Fig. 3 and unpublished data). By contrast, the amount of MyHC and none of the thick filaments components (i.e., MyLC1, MyLC2, and MyBP-C) decreased in ΔR-MuRF1$^{myc/myc}$ animals. This slower loss of MyHC is consistent with the hypothesis that the initial selective degradation of the thick filament–stabilizing proteins MyLC1, MyLC2, and MyBP-C enhances the accessibility of MyHC to ubiquitylation by MuRF1.

Unlike these thick filament components, at this time after denervation the thin filament components, actin, tropomyosin, and α-actinin were lost from the myofibril in a similar fashion in the MuRF1$^{myc/myc}$ and ΔR-MuRF1$^{myc/myc}$ animals (Fig. 6 A). Thus, although MuRF1 is required for the degradation and disassembly of the thick filaments during denervation atrophy, the thin filaments are degraded by a distinct mechanism that does not require MuRF1 or MuRF1-dependent ubiqutiylation of other components, but may involve another ubiquitin ligase.

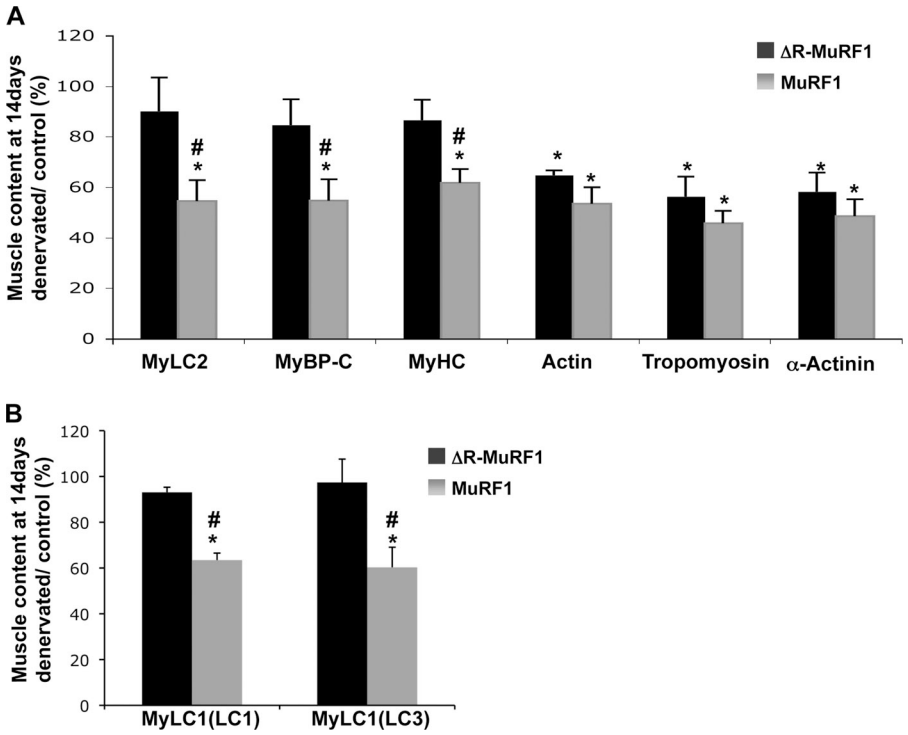

Figure 6. **MyHC is lost from the myofibril by a MuRF1-dependent mechanism 14 d after denervation.** The myofibrillar fraction from innervated muscles and ones denervated for 14 d from both MuRF1$^{myc/myc}$ and ΔR-MuRF1$^{myc/myc}$ mice were analyzed by SDS-PAGE, Coomassie blue staining (A), immunoblotting with specific antibodies as indicated (B), and densitometric measurement of the specific bands. The content of each myofibrillar protein in denervated muscle is presented as percentage of levels in control. Error bars represent SEM, $n = 3$. *, $P < 0.05$ denervation versus control. #, $P < 0.05$ denervation in MuRF1$^{myc/myc}$ versus ΔR-MuRF1$^{myc/myc}$ mice.

Discussion

The present findings clarify the critical role that MuRF1 plays in muscle atrophy. Although other ubiquitin ligases are also induced during atrophy (i.e., atrogin-1 [Gomes et al., 2001], which is also essential for rapid atrophy [Bodine et al., 2001], as well as E3α-II [Kwak et al., 2004]), MuRF1 is necessary for most of the increase in ubiquitin conjugates during denervation atrophy (Fig. 2). Thus, MuRF1 either ubiquitylates most proteins being degraded 10 d after denervation, or its actions allow other ligases to act. In either case, MuRF1 clearly is a very general ligase affecting many contractile (Table I), soluble, and nuclear proteins (unpublished data), as was also suggested by two-hybrid studies (Witt et al., 2005; Hirner et al., 2008). Moreover, our studies implicate ubiquitylation by MuRF1 in the selective loss of MyBP-C, MyLC1, and MyLC2, as well as the slower degradation of MyHC, and thereby in the disassembly and degradation of myofibrillar proteins, which is the defining feature of the atrophy process.

Inactivation of MuRF1's capacity to bind E2s by deletion of its Ring-finger motif attenuated atrophy and prevented the differential loss of MyBP-C, MyLC1, and MyLC2 from the myofibril (Fig. 3). Their selective loss is a new feature of atrophying muscles and seems to be of regulatory importance. Because these proteins appear to be critical in stabilizing the myofibril (see below), the reduced loss of MyHC in the ΔR-MuRF1$^{myc/myc}$ mice might be a direct consequence of the sparing of MyLC1, MyLC2, and MyBP-C. Also surprising were the findings that these components of the thick filaments are degraded sooner and by a distinct mechanism from the thin filament components, actin, tropomyosin, and α-actinin, whose degradation is independent of MuRF1.

Because MuRF1 is required for rapid atrophy, but not for normal muscle growth or function, identification of its substrates is essential to understand the mechanisms of protein loss. We have identified a number of myofibrillar components as novel substrates for MuRF1 in vivo, all of which are important for muscle integrity and contractile activity. Mutations in each of them cause severe disorders characterized by disarrayed myofibrils and compromised contractile function (Clark et al., 2002). Although cardiac Troponin-I was previously reported to be a MuRF1 substrate (Kedar et al., 2004), Troponin-I could not be immunoprecipitated with MuRF1 from these skeletal muscles and was not lost by a MuRF1-dependent mechanism after denervation. MyHC had been shown to accumulate in mice lacking MuRF1 and MuRF3 (Fielitz et al., 2007) and to be degraded in a MuRF1-dependent manner upon dexamethasone treatment of embryonic myotubes (Clarke et al., 2007). Accordingly, decreased content of MyHC by a MuRFl-dependent mechanism was clearly evident at 14 d denervation (Fig. 6). However, within the myofibril from innervated muscles, MyHC is not ubiquitylated by MuRF1 and is not a preferred substrate of MuRF1 even 10 d after denervation (Fig. 3).

It is noteworthy that these various myofibrillar proteins could be precipitated with GST-MuRF1 from the cytosolic fraction, and were ubiquitylated by pure MuRF1. Soluble pools of these myofibrillar components have been reported in chicken (Horvath and Gaetjens, 1972) and were found in the mouse muscle extracts (unpublished data). Possibly, these soluble components function either as precursors to the mature contractile apparatus or as components released during myofibrillar turnover, or may represent a fraction of myofibrillar proteins that are easily released upon homogenization (Etlinger et al., 1975). However, these proteins did not accumulate in the cytosol

during atrophy, when they were lost from the myofibril (unpublished data).

Although it has long been recognized that the major myofibrillar proteins are degraded by the ubiquitin–proteasome pathway during atrophy (Solomon and Goldberg, 1996), the identification of MuRF1 as the critical ligase that acts on the myofibrillar compartment (perhaps together with other E3s) suggests a role for ubiquitylation in disassembly of the myofibril. It is noteworthy that purified monomeric actin and MyHC were efficiently ubiquitylated by MuRF1, but not when associated with each other in the actomyosin complex or in the intact myofibril (Fig. 4, unpublished data). Previously, Solomon and Goldberg (1996) demonstrated in crude homogenates that the ubiquitin–proteasome system rapidly degrades monomeric actin and myosin, but this process was not demonstrable in the extracts, when these proteins were associated with each other in the actomyosin complex or a myofibril. These early findings suggested that during atrophy a mechanism may exist to release these components from the myofibril or to enhance the susceptibility of actin, myosin, and other myofibrillar proteins to ubiquitylation. However, based upon the present findings, it no longer seems necessary to postulate such a release system (see below).

MuRF1 could ubiquitylate these substrates together with UbcH1, which forms K-48–linked polyubiquitin chains, and UbcH13/Uev1, which forms processively K-63–linked chains, and UbcH5, which forms mixed chains (Kim et al., 2007) (Fig. 4). However, it is unclear which E2s function in proteolysis with MuRF1 or which types of ubiquitin chains it forms in normal or atrophying muscles. Although K-63–linked ubiquitin chains were believed to serve functions other than proteasomal degradation in vivo, recent findings indicate that K63 chains can target substrates to the proteasome in vitro and in vivo (Saeki et al., 2009). Also, the nature and content of the E2s can influence the rates of protein degradation and thus the rate of atrophy.

It is particularly intriguing that MyLC1, MyLC2, and MyBP-C are selectively degraded in a MuRF1-dependent manner after denervation (Fig. 3), and that these proteins, unlike MyHC and actin, are efficiently ubiquitylated by MuRF1 within the myofibril (Fig. 5 B, unpublished data). Thus, these critical stabilizing proteins can be substrates within the myofibril without dissociation or proteolytic processing. Furthermore, the susceptibility of MyHC to ubiquitylation and degradation is enhanced 14 d after denervation (Fig. 6 A), presumably because the levels of MyBP-C and MyLCs in the myofibril are reduced. Accordingly, myosin can be extracted from the cardiac thick filament only after MyBP-C content has been reduced by 20% (Kulikovskaya et al., 2007). By contrast, the thin filament components, actin, tropomyosin, and α-actinin, were lost from the myofibril 14 d after denervation by a mechanism that does not require MuRF1 or the MuRF1-dependent loss of MyBP-C and MyLCs. However, it is also possible that MuRF1 may target for degradation proteins associated within the Z-disk lattice because Filamin C was precipitated together with MuRF1 (Table I). Alternatively, another E3 induced in atrophy may promote disassembly of the Z-disk or thin filaments, and function in the ΔR-MuRF1 animals.

Although no reduction in the absolute levels of contractile proteins was demonstrable by these techniques until 10 d after denervation, their degradation must have been accelerated much sooner because the loss of proteins results from the integrated effects of enhanced proteolysis over time. Any small changes in myofibrillar content (e.g., 10–20% decreases) that occur sooner after denervation probably cannot be detected by the methods used here. Accordingly, our finding that MuRF1 is induced by 3 d after denervation (Fig. 5 A) implies that MuRF1 functions maximally early in atrophy (and before any loss of myofibrillar proteins is detectable). MuRF1 may promote the degradation of soluble cytosolic components, many of which associate with MuRF1 (unpublished data).

It is noteworthy that decreases in muscle mass can be demonstrated during the first week after denervation (Furuno et al., 1990) and do not seem attributable to MuRF1-dependent loss of myofibrillar components (Fig. 6 A). However, other E3s are induced rapidly during atrophy (e.g., atrogin-1) and may help accelerate degradation. Also, recent investigations have shown that autophagy is activated rapidly during denervation-atrophy and seems to promote destruction of mitochondria and cytosolic proteins, perhaps during the first week after denervation (Mammucari et al., 2007; Zhao et al., 2007; O'Leary and Hood, 2009), before any loss of myofibrillar myosin and actin can be detected.

Thus, during atrophy, MuRF1 seems to function at the initial steps of thick filament disassembly, apparently by selectively ubiquitylating certain key regulatory components, whose degradation should facilitate the breakdown of the remaining thick filament components. The extraction of these ubiquitylated regulatory proteins from the myofibril might be directly linked to their degradation by the 26S proteasome, whose 19S component catalyzes ATP-dependent unfolding and translocation of substrates into the core 20S proteasome (Smith et al., 2005). Alternatively, ATP-dependent extraction of these proteins may be catalyzed by the p97/VCP complex, which extracts ubiquitin-conjugated proteins from ER membranes in the ER-associated degradation pathway (Ye et al., 2001) and plays an important role in myofibril assembly (Janiesch et al., 2007). Additional evidence for a critical regulatory role of myofibrillar MyBP-C is that mRNAs for this protein also decrease selectively during denervation atrophy (unpublished data).

MyBP-C and MyLC2 are critical modulators of muscle contractility, and their loss may account for some of the alterations in contractile properties seen after denervation (Zorzato et al., 1989; Trachez et al., 1990). Extraction of MyBP-C from skinned fibers leads to an increase in the Ca^{2+} sensitivity of force development (Hofmann et al., 1991). Removal of myofibrillar MyLC2 has a similar effect on the Ca^{2+}-tension curve as removal of MyBP-C. Both proteins thus appear to reduce inappropriate contractions by decreasing the probability of the myosin heads binding to actin (Moss et al., 1983). In addition, in heart, increasing MyBP-C content enhances the ATPase activity of actomyosin but not if MyLC2 was removed, and this effect reappeared when MyLC2 was restored (Margossian, 1985).

Several days after denervation, the muscle's contractile properties change (i.e., there is a prolongation of the contraction and relaxation periods), apparently due to alterations in intracellular concentrations of Ca^{2+} (Zorzato et al., 1989) as well as

an increased myofibrillar Ca^{2+} sensitivity (Trachez et al., 1990). As noted above, extraction of MyBP-C or MyLC2 also leads to increased myofibrillar sensitivity to Ca^{2+}. Because Ca^{2+} is less efficiently pumped out of the cytosol of denervated muscle (Finol et al., 1981), the selective loss of these regulatory components might contribute to their altered contractile properties. Another characteristic of atrophied muscle is a progressive reduction in the twitch force. Because MyLC1 is required for full force production by muscle myosin (VanBuren et al., 1994), its selective loss (as well as subsequent loss of MyHC) should contribute to the loss of tension after denervation.

Although the ubiquitylation on the myofibril and selective degradation of the critical stabilizing proteins MyBP-C, MyLC1, and MyLC2 by MuRF1 is an attractive new mechanism for loss of the thick filaments, it remains to be proven that these sequential steps are essential for the loss of MyHC and rapid atrophy. It will also be important to establish the nature of the subsequent steps, which lead to a loss of thin filaments during atrophy and also during the slower turnover of myofibrillar components in normal muscle. This mechanism (ubiquitylation of key regulatory components in the myofibril) is very different from the frequent suggestion that the initial attack on the contractile apparatus is by endoproteases, such as caspases (Du et al., 2004) or calpains (Tidball and Spencer, 2002). Although such mechanisms may function in certain apoptotic conditions (Du et al., 2004), direct evidence that these proteases play an essential or primary role is lacking, and the present findings demonstrate a very different MuRF1-dependent mechanism that appears to function in vivo at the level of the myofibril.

Materials and methods

Antibodies and materials

Anti-Myc was purchased from Santa Cruz Biotechnology, Inc., anti-ubiquitin (clone FK2) from Biomol, anti-MyHC from Abcam, and anti-actin from Sigma-Aldrich. Anti-MyLC2 (developed by Donald A. Fischman) and anti-MyLC1 (developed by Frank E. Stockdale) were obtained from Developmental Studies Hybridoma Bank under the auspices of the NICHD (University of Iowa, Iowa City, IA). The MyBP-C antibody and the clone for MyBP-C expression in *Escherichia coli* were provided by Dr. Marion Greaser (University of Wisconsin-Madison, Madison, WI). MyLC, MyHC, actin, and actomyosin were purchased from Sigma-Aldrich. The MuRF1 antibody was raised against rat MuRF1 and was described previously by Bodine et al. (2001). UbcH1 and UbcH13/Uev1 E2-conjugating enzymes were purchased from Boston Biochem. UbcH5 clone for expression in *E. coli* was provided by Dr. Kazuhiro Iwai (Osaka City University, Osaka-shi, Japan). The GST-MuRF1 construct for expression in *E. coli* was described previously by Bodine et al. (2001). Glutathione Sepharose 4B was purchased from GE Healthcare and was used to immobilize GST-MuRF1.

Generation of knock-in mice

$MuRF1^{myc/myc}$ and $\Delta R\text{-}MuRF1^{myc/myc}$ mice were generated using VelociGene Technology (Valenzuela et al., 2003). In brief, the targeting vectors were constructed by replacing the genomic sequence coding from ATG-S110 of mouse MuRF1 (exons 1 and 2) with a DNA fragment containing the 3xMyc epitope (36 amino acids) fused to the corresponding replaced region, including or excluding the Ring-finger domain (C23-C78, deletion of 55 amino acids), followed by a floxed neomycin resistance cassette. The NotI-linearized targeting vectors were electroporated into R1 embryonic stem (ES) cells as previously described (Valenzuela et al., 2003). Upon homologous recombination of the $MuRF1^{+/myc\text{-}neo}$ or $\Delta R\text{-}MuRF1^{+/myc\text{-}neo}$ allele in ES cells, the neomycin resistance was removed using a Cre expression vector. Chimeric mice, generated by injection of targeted ES clones into C57BL/6 blastocysts, were mated to C57BL/6 to transmit into the germ line, and the resulting heterozygous mice were mated to generate homozygous $MuRF1^{myc/myc}$ and $\Delta R\text{-}MuRF1^{myc/myc}$ for all experiments. Targeted replacement of *MuRF1* for *Myc-MuRF1* and *Myc-ΔR-MuRF1* resulted in the removal of the genomic sequence between the first two coding exons. A real-time PCR-based loss of native allele (LONA) assay using probes near the 5′ and 3′ ends of the deletion was use to screen ES cells and mouse-tail genotyping. In addition, selected mice were genotyped by PCR using oligos flanking the region where the triple Myc-encoding sequence (108 base pairs) was inserted using the oligos 5′-CTGAGAGGGCCAAATCTTT-GAGGC-3′ and 5′-AGCTGCTTCTCCAGGTTCTCCATAG-3′.

Fractionation of muscle tissue

Mouse gastrocnemius muscles were homogenized on ice for 30 s in 19 volumes of homogenization buffer (20 mM Tris-HCl, pH 7.2, 5 mM EGTA, 100 mM KCl, and 1% Triton X-100), and incubated for 1 h with gentle agitation. After centrifugation at 3,000 *g* for 30 min, the supernatant (i.e., cytosolic fraction) was stored at −80°C. The pellet (myofibrils) was homogenized once in 20 volumes of homogenization buffer and twice in wash buffer (20 mM Tris-HCl, pH 7.2, 100 mM KCl, and 1 mM DTT). Before the final centrifugation (3,000 *g* for 10 min at 4°C) the resuspended pellet was filtered through a nylon cloth. The final pellet was resuspended in storage buffer (20 mM Tris-HCl, pH 7.2, 100 mM KCl, 1 mM DTT, and 20% glycerol) and kept at −80°C. All buffers contained a protease inhibitor mix (10 µg/ml leupeptin, 10 µg/ml pepstatin, 3 mM benzamidine, 1 µg/ml trypsin inhibitor, and 1 mM PMSF). Isolated myofibrils (2.5 µg per well) were separated on SDS-PAGE for Coomassie blue staining.

Immunoprecipitation

The cytosolic fraction (6 mg) of gastrocnemius muscle from $\Delta R\text{-}MuRF1^{myc/myc}$ mice was precleared with mouse IgG and Protein L-Agarose for 1 h at 4°C. Myc-ΔR-MuRF1 was immunoprecipitated with anti Myc coupled to beads overnight at 4°C. In parallel, a homogenate of the gastrocnemius muscle from wild-type mice was precleared with immobilized GST for 1 h at 4°C, and then immobilized GST-MuRF1 was added for overnight incubation at 4°C. Immunoprecipitated material was washed twice with each of the following buffers: LSB (50 mM Tris-Cl, pH 8, 0.1% Triton X-100, and 5 mM EDTA), MSB (50 mM Tris-Cl, pH 8, 150 mM NaCl, 0.1% SDS, 0.1% Triton X-100, and 5 mM EDTA), and HSB (50 mM Tris-Cl, pH 8, 500 mM NaCl, 0.1% SDS, 1% Triton X-100, 5 mM EGTA, and 5 mM EDTA) before a 10-min heating at 70°C in sample buffer (Invitrogen) and 50 mM DTT.

Protein identification by mass spectrometry

Purified samples were resolved on SDS-PAGE and visualized by Coomassie blue. The gel was cut into eight regions, excised and subjected to in-gel trypsin digestion. Tryptic peptides were extracted from the gel and analyzed by liquid chromatography MS/MS (LC-MS/MS). Peptides were separated using a 37-min gradient ranging from 4 to 27% (vol/vol) acetonitrile in 0.1% (vol/vol) trifluoroacetic acid in a microcapillary (125 µm x 18 cm) column packed with C18 reverse-phase material (Magic C18AQ, 5-µm particles, 200 Å pore size; Michrom Bioresources) and on-line analyzed on The LTQ Orbitrap XL hybrid FTMS (ThermoElectron). For each cycle, one full MS scan acquired on the Orbitrap at high mass resolution was followed by ten MS/MS spectra on the linear ion trap XL from the ten most abundant ions. MS/MS spectra were searched using the Sequest algorithm against mouse NCI protein database. All peptide matches were filtered based on mass deviation, Xcorr and dCorr, miscleavages, peptide length to get <1% false discover rate.

Immunoblotting

Cytosolic or myofibrillar fractions from gastrocnemius muscles as well as the in vitro ubiquitylation reactions were resolved by SDS-PAGE, transferred onto PVDF membranes, and immunoblotted with specific antibodies and secondary antibodies conjugated to alkaline phosphatase.

In vitro ubiquitylation assays

Ubiquitylation assays of pure proteins (1 µM MyLC, MyBP-C, or actin, and 100 nM MyHC) and actomyosin (5 µg for MyLC and 0.13 µg for MyHC) were performed for 90 min at 37°C in 20-µl mixtures containing 22.5 nM E1, 0.75 µM E2, 0.4 µM MuRF1, and 59 µM ubiquitin in reaction buffer (2 mM ATP, 20 mM Tris-HCl, pH 7.6, 20 mM KCl, 5 mM $MgCl_2$, and 1 mM DTT). Ubiquitylation of isolated washed myofibrils (4 µg for MyBP-C, 1.11 µg for MyLC) was performed as described above except that His-ubiquitin was used, and the E2 was UbcH1 in all experiments. After incubation at 1,400 rpm for 90 min at 37°C, myofibrils were solubilized by the addition of 12.5 µl of 1.6x solubilization solution (0.8 M KCl, 80 mM Tris, 0.16 mM $MgCl_2$, 16 mM ATP, and 8 M Urea, pH 8) per 20-µl reaction and incubated for 30 min at 4°C

with agitation. Ubiquitylated myofibrillar proteins were purified with Ni-beads. All solutions were prepared shortly before use.

Statistical analysis and image acquisition

Data are presented as means and error bars indicate SEM. The statistical significance was accessed by paired Student's *t* test. Images were processed by Adobe Photoshop CS3, version 10.0.1.

Online supplemental material

Figure S1 shows a representative gel of MuRF1-bound muscle proteins before mass spectrometry analysis. Figure S2 shows a representative genotyping data of the knock-in mice using the LONA assay, and PCR analysis of tail genomic DNA showing the products from the WT and targeted alleles. Figure S3 shows that endogenous MuRF1, Myc-MuRF1, and Myc-ΔR-MuRF1 proteins are found mainly in the cytosolic fraction and not in myofibrils. Figure S4 shows a representative Coomassie blue–stained gel of isolated myofibrils, which was used for densitometric measurement of specific protein bands. Figure S5 shows differential loss of MyBP-C and MyLC1 and MyLC2 from the myofibril upon food deprivation, and in vitro ubiquitylation of actin by MuRF1. Online supplemental material is available at http://www.jcb.org/cgi/content/full/jcb.200901052/DC1.

We thank all at Regeneron Pharmaceuticals for their assistance and support, especially Trevor Stitt. We acknowledge the VelociGene group for generating targeted ES cells, blastocyst injections, and genotyping of the mice.

This project was supported by grants from the Muscular Dystrophy Association and Ellison Medical Foundation to A.L. Goldberg, a stipend to S. Cohen from the International Sephardic Education Foundation (ISEF), and a National Institutes of Health grant (F32 AR054699) to J.J. Brault.

Submitted: 12 January 2009
Accepted: 13 May 2009

References

Bodine, S.C., E. Latres, S. Baumhueter, V.K. Lai, L. Nunez, B.A. Clarke, W.T. Poueymirou, F.J. Panaro, E. Na, K. Dharmarajan, et al. 2001. Identification of ubiquitin ligases required for skeletal muscle atrophy. *Science.* 294:1704–1708.

Centner, T., J. Yano, E. Kimura, A.S. McElhinny, K. Pelin, C.C. Witt, M.L. Bang, K. Trombitas, H. Granzier, C.C. Gregorio, et al. 2001. Identification of muscle specific ring finger proteins as potential regulators of the titin kinase domain. *J. Mol. Biol.* 306:717–726.

Chen, Z., W. Huang, T. Dahme, W. Rottbauer, M.J. Ackerman, and X. Xu. 2008. Depletion of zebrafish essential and regulatory myosin light chains reduces cardiac function through distinct mechanisms. *Cardiovasc. Res.* 79:97–108.

Clark, K.A., A.S. McElhinny, M.C. Beckerle, and C.C. Gregorio. 2002. Striated muscle cytoarchitecture: an intricate web of form and function. *Annu. Rev. Cell Dev. Biol.* 18:637–706.

Clarke, B.A., D. Drujan, M.S. Willis, L.O. Murphy, R.A. Corpina, E. Burova, S.V. Rakhilin, T.N. Stitt, C. Patterson, E. Latres, and D.J. Glass. 2007. The E3 ligase MuRF1 degrades myosin heavy chain protein in dexamethasone-treated skeletal muscle. *Cell Metab.* 6:376–385.

Du, J., Z. Hu, and W.E. Mitch. 2005. Molecular mechanisms activating muscle protein degradation in chronic kidney disease and other catabolic conditions. *Eur. J. Clin. Invest.* 35:157–163.

Du, J., X. Wang, C. Miereles, J.L. Bailey, R. Debigare, B. Zheng, S.R. Price, and W.E. Mitch. 2004. Activation of caspase-3 is an initial step triggering accelerated muscle proteolysis in catabolic conditions. *J. Clin. Invest.* 113:115–123.

Etlinger, J.D., R. Zak, D.A. Fischman, and M. Rabinowitz. 1975. Isolation of newly synthesised myosin filaments from skeletal muscle homogenates and myofibrils. *Nature.* 255:259–261.

Fielitz, J., M.S. Kim, J.M. Shelton, S. Latif, J.A. Spencer, D.J. Glass, J.A. Richardson, R. Bassel-Duby, and E.N. Olson. 2007. Myosin accumulation and striated muscle myopathy result from the loss of muscle RING finger 1 and 3. *J. Clin. Invest.* 117:2486–2495.

Finol, H.J., D.M. Lewis, and R. Owens. 1981. The effects of denervation on contractile properties or rat skeletal muscle. *J. Physiol.* 319:81–92.

Furuno, K., M.N. Goodman, and A.L. Goldberg. 1990. Role of different proteolytic systems in the degradation of muscle proteins during denervation atrophy. *J. Biol. Chem.* 265:8550–8557.

Goll, D.E., V.F. Thompson, R.G. Taylor, and J.A. Christiansen. 1992. Role of the calpain system in muscle growth. *Biochimie.* 74:225–237.

Gomes, M.D., S.H. Lecker, R.T. Jagoe, A. Navon, and A.L. Goldberg. 2001. Atrogin-1, a muscle-specific F-box protein highly expressed during muscle atrophy. *Proc. Natl. Acad. Sci. USA.* 98:14440–14445.

Hatakeyama, S., and K.I. Nakayama. 2003. U-box proteins as a new family of ubiquitin ligases. *Biochem. Biophys. Res. Commun.* 302:635–645.

Hirner, S., C. Krohne, A. Schuster, S. Hoffmann, S. Witt, R. Erber, C. Sticht, A. Gasch, S. Labeit, and D. Labeit. 2008. MuRF1-dependent regulation of systemic carbohydrate metabolism as revealed from transgenic mouse studies. *J. Mol. Biol.* 379:666–677.

Hofmann, P.A., H.C. Hartzell, and R.L. Moss. 1991. Alterations in Ca2+ sensitive tension due to partial extraction of C-protein from rat skinned cardiac myocytes and rabbit skeletal muscle fibers. *J. Gen. Physiol.* 97:1141–1163.

Horvath, B.Z., and E. Gaetjens. 1972. Immunochemical studies on the light chains from skeletal muscle myosin. *Biochim. Biophys. Acta.* 263:779–793.

Jackman, R.W., and S.C. Kandarian. 2004. The molecular basis of skeletal muscle atrophy. *Am. J. Physiol. Cell Physiol.* 287:C834–C843.

Jang, J.H. 2004. FIGC, a novel FGF-induced ubiquitin-protein ligase in gastric cancers. *FEBS Lett.* 578:21–25.

Janiesch, P.C., J. Kim, J. Mouysset, R. Barikbin, H. Lochmuller, G. Cassata, S. Krause, and T. Hoppe. 2007. The ubiquitin-selective chaperone CDC-48/p97 links myosin assembly to human myopathy. *Nat. Cell Biol.* 9:379–390.

Kedar, V., H. McDonough, R. Arya, H.H. Li, H.A. Rockman, and C. Patterson. 2004. Muscle-specific RING finger 1 is a bona fide ubiquitin ligase that degrades cardiac troponin I. *Proc. Natl. Acad. Sci. USA.* 101:18135–18140.

Kim, H.T., K.P. Kim, F. Lledias, A.F. Kisselev, K.M. Scaglione, D. Skowyra, S.P. Gygi, and A.L. Goldberg. 2007. Certain pairs of ubiquitin-conjugating enzymes (E2s) and ubiquitin-protein ligases (E3s) synthesize nondegradable forked ubiquitin chains containing all possible isopeptide linkages. *J. Biol. Chem.* 282:17375–17386.

Koegl, M., T. Hoppe, S. Schlenker, H.D. Ulrich, T.U. Mayer, and S. Jentsch. 1999. A novel ubiquitination factor, E4, is involved in multiubiquitin chain assembly. *Cell.* 96:635–644.

Kulikovskaya, I., G.B. McClellan, R. Levine, and S. Winegrad. 2007. Multiple forms of cardiac myosin-binding protein C exist and can regulate thick filament stability. *J. Gen. Physiol.* 129:419–428.

Kwak, K.S., X. Zhou, V. Solomon, V.E. Baracos, J. Davis, A.W. Bannon, W.J. Boyle, D.L. Lacey, and H.Q. Han. 2004. Regulation of protein catabolism by muscle-specific and cytokine-inducible ubiquitin ligase E3alpha-II during cancer cachexia. *Cancer Res.* 64:8193–8198.

Lecker, S.H., V. Solomon, W.E. Mitch, and A.L. Goldberg. 1999. Muscle protein breakdown and the critical role of the ubiquitin-proteasome pathway in normal and disease states. *J. Nutr.* 129:227S–237S.

Lecker, S.H., A.L. Goldberg, and W.E. Mitch. 2006. Protein degradation by the ubiquitin-proteasome pathway in normal and disease states. *J. Am. Soc. Nephrol.* 17:1807–1819.

Mammucari, C., G. Milan, V. Romanello, E. Masiero, R. Rudolf, P. Del Piccolo, S.J. Burden, R. Di Lisi, C. Sandri, J. Zhao, et al. 2007. FoxO3 controls autophagy in skeletal muscle in vivo. *Cell Metab.* 6:458–471.

Margossian, S.S. 1985. Reversible dissociation of dog cardiac myosin regulatory light chain 2 and its influence on ATP hydrolysis. *J. Biol. Chem.* 260:13747–13754.

McElhinny, A.S., K. Kakinuma, H. Sorimachi, S. Labeit, and C.C. Gregorio. 2002. Muscle-specific RING finger-1 interacts with titin to regulate sarcomeric M-line and thick filament structure and may have nuclear functions via its interaction with glucocorticoid modulatory element binding protein-1. *J. Cell Biol.* 157:125–136.

Moss, R.L., A.E. Swinford, and M.L. Greaser. 1983. Alterations in the Ca2+ sensitivity of tension development by single skeletal muscle fibers at stretched lengths. *Biophys. J.* 43:115–119.

Munoz, K.A., S. Satarug, and M.E. Tischler. 1993. Time course of the response of myofibrillar and sarcoplasmic protein metabolism to unweighting of the soleus muscle. *Metabolism.* 42:1006–1012.

Offer, G., H. Baker, and L. Baker. 1972. Interaction of monomeric and polymeric actin with myosin subfragment 1. *J. Mol. Biol.* 66:435–444.

O'Leary, M.F., and D.A. Hood. 2009. Denervation-induced oxidative stress and autophagy signaling in muscle. *Autophagy.* 5:230–231.

Qiu, X.B., and A.L. Goldberg. 2002. Nrdp1/FLRF is a ubiquitin ligase promoting ubiquitination and degradation of the epidermal growth factor receptor family member, ErbB3. *Proc. Natl. Acad. Sci. USA.* 99:14843–14848.

Rodrigo-Brenni, M.C., and D.O. Morgan. 2007. Sequential E2s drive polyubiquitin chain assembly on APC targets. *Cell.* 130:127–139.

Rottbauer, W., G. Wessels, T. Dahme, S. Just, N. Trano, D. Hassel, C.G. Burns, H.A. Katus, and M.C. Fishman. 2006. Cardiac myosin light chain-2: a novel essential component of thick-myofilament assembly and contractility of the heart. *Circ. Res.* 99:323–331.

Sacheck, J.M., J.P. Hyatt, A. Raffaello, R.T. Jagoe, R.R. Roy, V.R. Edgerton, S.H. Lecker, and A.L. Goldberg. 2007. Rapid disuse and denervation atrophy involve transcriptional changes similar to those of muscle wasting during systemic diseases. *FASEB J.* 21:140–155.

Saeki, Y., T. Kudo, T. Sone, Y. Kikuchi, H. Yokosawa, A. Toh-e, and K. Tanaka. 2009. Lysine 63-linked polyubiquitin chain may serve as a targeting signal for the 26S proteasome. *EMBO J.* 28:359–371.

Smith, D.M., G. Kafri, Y. Cheng, D. Ng, T. Walz, and A.L. Goldberg. 2005. ATP binding to PAN or the 26S ATPases causes association with the 20S proteasome, gate opening, and translocation of unfolded proteins. *Mol. Cell.* 20:687–698.

Solomon, V., and A.L. Goldberg. 1996. Importance of the ATP-ubiquitin-proteasome pathway in the degradation of soluble and myofibrillar proteins in rabbit muscle extracts. *J. Biol. Chem.* 271:26690–26697.

Tidball, J.G., and M.J. Spencer. 2002. Expression of a calpastatin transgene slows muscle wasting and obviates changes in myosin isoform expression during murine muscle disuse. *J. Physiol.* 545:819–828.

Trachez, M.M., R.T. Sudo, and G. Suarez-Kurtz. 1990. Alterations in the functional properties of skinned fibers from denervated rabbit skeletal muscle. *Am. J. Physiol.* 259:C503–C506.

Valenzuela, D.M., A.J. Murphy, D. Frendewey, N.W. Gale, A.N. Economides, W. Auerbach, W.T. Poueymirou, N.C. Adams, J. Rojas, J. Yasenchak, et al. 2003. High-throughput engineering of the mouse genome coupled with high-resolution expression analysis. *Nat. Biotechnol.* 21:652–659.

VanBuren, P., G.S. Waller, D.E. Harris, K.M. Trybus, D.M. Warshaw, and S. Lowey. 1994. The essential light chain is required for full force production by skeletal muscle myosin. *Proc. Natl. Acad. Sci. USA.* 91:12403–12407.

Weydert, A., P. Barton, A.J. Harris, C. Pinset, and M. Buckingham. 1987. Developmental pattern of mouse skeletal myosin heavy chain gene transcripts in vivo and in vitro. *Cell.* 49:121–129.

Wing, S.S., A.L. Haas, and A.L. Goldberg. 1995. Increase in ubiquitin-protein conjugates concomitant with the increase in proteolysis in rat skeletal muscle during starvation and atrophy denervation. *Biochem. J.* 307(Pt 3): 639–645.

Witt, C.C., S.H. Witt, S. Lerche, D. Labeit, W. Back, and S. Labeit. 2008. Cooperative control of striated muscle mass and metabolism by MuRF1 and MuRF2. *EMBO J.* 27:350–360.

Witt, S.H., H. Granzier, C.C. Witt, and S. Labeit. 2005. MURF-1 and MURF-2 target a specific subset of myofibrillar proteins redundantly: towards understanding MURF-dependent muscle ubiquitination. *J. Mol. Biol.* 350:713–722.

Yang, Q., A. Sanbe, H. Osinska, T.E. Hewett, R. Klevitsky, and J. Robbins. 1998. A mouse model of myosin binding protein C human familial hypertrophic cardiomyopathy. *J. Clin. Invest.* 102:1292–1300.

Ye, Y., H.H. Meyer, and T.A. Rapoport. 2001. The AAA ATPase Cdc48/p97 and its partners transport proteins from the ER into the cytosol. *Nature.* 414:652–656.

Zhao, J., J.J. Brault, A. Schild, P. Cao, M. Sandri, S. Schiaffino, S.H. Lecker, and A.L. Goldberg. 2007. FoxO3 coordinately activates protein degradation by the autophagic/lysosomal and proteasomal pathways in atrophying muscle cells. *Cell Metab.* 6:472–483.

Zorzato, F., P. Volpe, E. Damiani, D. Quaglino Jr., and A. Margreth. 1989. Terminal cisternae of denervated rabbit skeletal muscle: alterations of functional properties of Ca2+ release channels. *Am. J. Physiol.* 257:C504–C511.